# HIGH-FREQUENCY SOUND NEAR THE CURIE POINT OF FERROMAGNETS

V. G. KAMENSKIĬ

L. D. Landau Institute of Theoretical Physics, USSR Academy of Sciences

Submitted July 23, 1970

Zh. Eksp. Teor. Fiz. 59, 2244–2251 (December, 1970)

Propagation of sound with frequency larger than the reciprocal relaxation time of magnons in ferrodielectrics near the Curie point is investigated by successive approximations for self-consistent field.[6] It is shown that in this case the damping of the sound is determined by the interaction of the phonons with the spin waves. The frequency and temperature dependences of the magnetic absorption of sound obtained in this manner are compared with the corresponding dependences for the absorption of sound by thermal phonons, and also with the case of low temperatures.

IF it is assumed that the influence of the inhomogeneities, impurities, and domain walls on the propagation of sound in a ferrodielectric is negligible, then the process responsible for the absorption of energy of sound waves is their interaction with thermal phonons and the spin system. It is of interest to separate effects connected with the magnetic interaction and to compare them subsequently with effects corresponding to thermal phonons.

The question of propagation of sound in ferromagnets was discussed in a number of papers.[1-5] In [1,2] they considered different processes of interaction of sound with a spin system. It was shown that for sufficiently high temperatures, the principal role is played by processes of production and absorption of phonons by spin waves (magnons), corresponding to the joining of a sound quantum to a thermal magnon under the condition that simultaneous satisfaction of the energy and momentum conservation laws is possible. The decay of a phonon into two spin waves and the annihilation of two spin waves with formation of a phonon is the result of relativistic effects, and therefore the probabilities of these processes are low and become significant only for $T \ll \Theta_0^2/\Theta_C$ ($\Theta_0$ and $\Theta_C$ are the Debye and Curie temperatures, respectively). It is likewise unnecessary to take into account two-phonon processes of next order of smallness.

In all the cited papers, however, the temperatures considered were much lower than $\Theta_C$. In this connection, definite interest attaches to the case $T \gtrsim \Theta_C$. It is natural to expect that near the critical point the propagation of the sound will have a number of characteristic features peculiar to the region of phase transitions.

To describe ferrodielectrics in this temperature region, we shall use the diagram technique for systems with spin-spin interaction, developed by Vaks, Larkin, and Pikin.[6] This technique constitutes a series of successive approximations of the self-consistent field method, and is suitable for ferromagnets with a large interaction radius. In [7] this method was used to show that in a Heisenberg ferromagnet there exist long-wave spin waves at all $T < \Theta_C$, and a criterion which the wave vectors of these waves must satisfy was obtained.

Magnetic damping of sound at temperatures close to the transition temperature is determined by the interaction of the phonons with the spin waves and by the spin fluctuations. In the present paper we obtain an expression for the damping of high-frequency sound near $\Theta_C$. The obtained frequency and temperature dependences of the magnetic absorption of the sound are compared with the corresponding dependences of the absorption of sound by thermal phonons,[8,9] and also with the case of low temperatures.[3]

We consider an ideal Heisenberg ferromagnet with an arbitrary exchange interaction between the spins, with a Hamiltonian in the form

$$\hat{\mathcal{H}} = -\mu H \sum_{\mathbf{r}} S_{\mathbf{r}}^z - {}^1/_2 \sum_{\mathbf{r}\neq\mathbf{r}'} V(\mathbf{r}-\mathbf{r}')\mathbf{S}_{\mathbf{r}}\mathbf{S}_{\mathbf{r}'}. \qquad (1)$$

Here $\mathbf{S}_{\mathbf{r}}$ is the spin operator of the atom, which is assumed to be fixed in the crystal-lattice site, $\mathbf{r}$ is the coordinate of the site, $V(\mathbf{r}-\mathbf{r}')$ is the effective potential of the interaction between the spins, H is the external magnetic field and is directed along the z axis, and $\mu$ is the Bohr magneton. The summation is over all the lattice sites.

The connection between the spins and lattice vibrations in the Hamiltonian (1) is given by the terms that arise when the interaction potential is expanded in terms of the displacements of the sites:

$$V(\mathbf{r}-\mathbf{r}') = V^0(\mathbf{r}-\mathbf{r}') + [\nabla_{\mathbf{r}} V(\mathbf{r}-\mathbf{r}')]^0 \mathbf{u}_{\mathbf{r}} + [\nabla_{\mathbf{r}'} V(\mathbf{r}-\mathbf{r}')]^0 \mathbf{u}_{\mathbf{r}'}, \quad (2)$$

where the zero index corresponds to quantities taken at the equilibrium values of $\mathbf{r}$ and $\mathbf{r}'$, and $\mathbf{u}_{\mathbf{r}}$ is the displacement of the corresponding lattice site. We shall henceforth omit the zero index where there is no danger of misunderstanding.

To construct the successive approximations, it is convenient to separate in the Hamiltonian the interaction with average spin $\langle \mathbf{S}\rangle$. Substituting (2) in (1) and recognizing that

$$V(\mathbf{r}-\mathbf{r}') = V(\mathbf{r}'-\mathbf{r}),$$

$$\sum_{\mathbf{r}\neq\mathbf{r}'} \mathbf{u}_{\mathbf{r}}\nabla_{\mathbf{r}} V(\mathbf{r}-\mathbf{r}') = \sum_{\mathbf{r}} \mathbf{u}_{\mathbf{r}}\nabla_{\mathbf{r}} \sum_{\mathbf{r}'} V(\mathbf{r}-\mathbf{r}') \equiv 0,$$

$$\sum_{\mathbf{r}\neq\mathbf{r}'} \mathbf{u}_{\mathbf{r}}\mathbf{S}_{\mathbf{r}}\nabla_{\mathbf{r}} V(\mathbf{r}-\mathbf{r}') = \sum_{\mathbf{r}} \mathbf{u}_{\mathbf{r}}\mathbf{S}_{\mathbf{r}}\nabla_{\mathbf{r}} \sum_{\mathbf{r}'} V(\mathbf{r}-\mathbf{r}') \equiv 0,$$

we obtain

$$\hat{\mathcal{H}} = \hat{\mathcal{H}}_0 + \hat{\mathcal{H}}_{\rm int}, \qquad (1')$$

where

$$\hat{\mathcal{H}}_0 = \frac{NV_0\langle S\rangle^2}{2} - \sum_{\mathbf{r}} \mathbf{S}_{\mathbf{r}}(V_0\langle \mathbf{S}\rangle + \mu\mathbf{H}),$$

$$\hat{\mathscr{H}}_{\text{int}} = -{}^1/_2 \sum_{\mathbf{r}\neq\mathbf{r}'} V(\mathbf{r}-\mathbf{r}')(\mathbf{S}_\mathbf{r}-\langle\mathbf{S}\rangle)(\mathbf{S}_{\mathbf{r}'}-\langle\mathbf{S}\rangle) - \sum_{\mathbf{r}\neq\mathbf{r}'} \langle\mathbf{S}\rangle \mathbf{u}_\mathbf{r}\nabla_\mathbf{r} V(\mathbf{r}-\mathbf{r}')(S_{\mathbf{r}'}^z-\langle\mathbf{S}\rangle) - \sum_{\mathbf{r}\neq\mathbf{r}'} \mathbf{u}_\mathbf{r}\nabla_\mathbf{r} V(\mathbf{r}-\mathbf{r}')(\mathbf{S}_\mathbf{r}-\langle\mathbf{S}\rangle)(\mathbf{S}_{\mathbf{r}'}-\langle\mathbf{S}\rangle);$$

here N is the number of sites, and $V_0 = \sum_\mathbf{r} V^0(\mathbf{r})$.

In the zeroth approximation, which is obtained when $\hat{\mathscr{H}}_{\text{int}}$ is neglected, the spins and the phonons do not interact. For the spin system, this case corresponds to the zeroth approximation of the self-consistent field, and the average spin $\langle\mathbf{S}\rangle \equiv \langle\mathbf{S}^z\rangle$ is given, as usual, by the expression

$$\langle S^z\rangle = \frac{y-\beta\mu H}{\beta V_0} = b(y), \tag{3}$$

where $\beta = 1/T$, $y = \beta(V_0\langle S^z\rangle + \mu H)$, and $b(y)$ is a function connected with the Brillouin function $B_S(y)$:

$$b(y) = \frac{\operatorname{Sp}[S^z e^{S^z y}]}{\operatorname{Sp} e^{S^z y}} = SB_S(y) = \left(S+\frac{1}{2}\right)\operatorname{cth}\left[\left(S+\frac{1}{2}\right)y\right] - \frac{1}{2}\operatorname{cth}\frac{y}{2}.$$

To find the next approximations, we shall use the temperature diagram technique developed by Vaks, Larkin, and Pikin.[6] The corrections to the thermodynamic functions and the Green's function of the phonons $D(\mathbf{r}, \tau; \mathbf{r}', \tau') = -\langle \hat{T}\tilde{u}(\mathbf{r}, \tau)\tilde{u}(\mathbf{r}', \tau')\rangle$, where $\tilde{u}(\mathbf{r}, \tau)$ is the displacement operator, will be represented by a set of different connected diagrams, each of which can be represented in the form of single-cell blocks connected by the interaction lines $V(\mathbf{r}-\mathbf{r}')$ and $\nabla_\mathbf{r} V(\mathbf{r}-\mathbf{r}')$ and by the phonon lines. Each interaction line joins the vertices of different blocks, either $S^z$ with $S^z$, or $S^+$ with $S^-$, where $S^\pm = (S^x \pm iS^y)/\sqrt{2}$.

We shall represent the blocks $\Gamma_{nm}$, which contains n spin operators and m phonon operators (we note, incidentally, that the number of operators $S^+$ in the block should always coincide with the number of operators $S^-$), by a point with n outgoing interaction lines and m phonon lines. To each of these lines there corresponds a definite frequency and momentum. The conservation laws are satisfied in each block. Figure 1 shows several typical blocks. The calculation of single-cell blocks is carried out in the same manner as in [6]. The Fourier component of a single-cell block $\Gamma_{n0}$ with outgoing interaction lines (e.g., diagrams a and b of Fig. 1) is given by the expression

$$\Gamma_{n0}^{\alpha_1,\ldots,\alpha_n}(\omega_1,\ldots,\omega_n) = T^n \int_0^\beta \prod_{j=1}^n d\tau_j \exp(i\omega_j\tau_j) \times\left[\left\langle \hat{T}\prod_{j=1}^n S^{\alpha_j}(\tau_j)\right\rangle - \prod_{m_1+\cdots+m_k=n} \Gamma_{m_1}^{\alpha_1\ldots}\Gamma_{m_2\ldots}^{\ldots}\Gamma_{m_k}^{\ldots\alpha_n}\right]. \tag{4}$$

Here $S^\alpha(\tau) = \exp(\tilde{\mathscr{H}}_0\tau)S^\alpha\exp(-\tilde{\mathscr{H}}_0\tau)$, $\tilde{\mathscr{H}}_0 = -yTS^z$, $\hat{T}$ is the T-ordering symbol, $i\omega_m = 2\pi i m T$ are the imaginary frequencies of the temperature diagram technique, [10] the mean value $\langle\ldots\rangle$ denotes $\operatorname{Sp}\rho_0(\ldots)$ with $\rho_0 = \exp(-\beta\tilde{\mathscr{H}}_0)[\operatorname{Sp}\exp(-\beta\tilde{\mathscr{H}}_0)]^{-1}$. The second term in the right-hand side of (4) represents the sum of products of all the possible blocks of smaller order. In the final analysis, the $\Gamma_{n0}$ are expressed in accordance with the rules indicated in [6] in terms of Green's functions defined as follows:

$$G(\omega_n) = 1/(y - i\beta\omega_n).$$

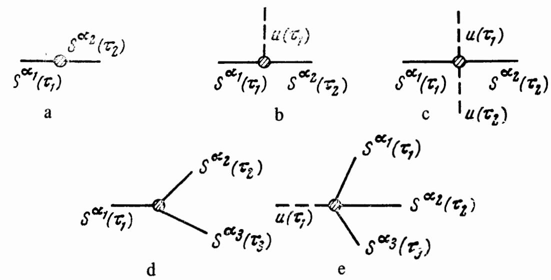

FIG. 1. Single-cell block.

In addition to the single-cell blocks of the type described above, there are also blocks $\Gamma_{nm}$ (see, e.g., diagrams b, c, and e of Fig. 1) with m outgoing phonon lines. It can be shown that the expressions for the Fourier components of such blocks are obtained from expressions for the blocks $\Gamma_{n0}$ of the same order in n, by making a suitable interchange of frequencies. If in the block $\Gamma_{nm}$ there are operators $S^{\alpha_j}(\tau_j)$ and $\tilde{u}(\tau_j)$ with coinciding temporal arguments, then to obtain its Fourier component it is necessary to replace $\omega_j$ in (4) by $\omega_j + \Omega_j$, where $\Omega_j$ is the frequency of the corresponding phonon line. Thus, for example, the diagram a of Fig. 1, with $\alpha_1$ and $\alpha_2$ having values "+" and "−", respectively, correspond to the expression

$$\Gamma_{20}^{+-}(\omega_1, \omega_2) = b(y)G(\omega_1)\delta(\omega_1-\omega_2),$$

while diagram b with the same $\alpha_1$ and $\alpha_2$ corresponds to the expression

$$\Gamma_{21}^{+-}(\omega_1, \omega_2, \Omega_1) = b(y)G(\omega_1+\Omega_1)\delta(\omega_1+\Omega_1-\omega_2).$$

In calculating the contributions corresponding to different diagrams, one sums over the internal frequencies and momenta. The result of the summation over the momentum is an expression proportional to $r_0^{-3} = (a/R_0)^3$, where $R_0$ is the average interaction radius and a is the cell dimension, so that the correction of order $l$ in the expansion in $r_0^{-3}$ will be represented by the aggregate of all possible connected diagrams containing $l$ closed loops.

The Dyson equation for the phonon Green's function (we shall consider only longitudinal phonons) has in the momentum representation the form

$$D^{-1}(\mathbf{k}, i\Omega_m) = D^{(0)-1}(\mathbf{k}, i\Omega_m) - \Pi(\mathbf{k}, i\Omega_m), \tag{5}$$

where $\Pi(\mathbf{k}, i\Omega_m)$ is the irreducible self-energy part and

$$D^{(0)}(\mathbf{k}, i\Omega_m) = -1/M[\Omega_m^2 + \Omega_0^2(\mathbf{k})]$$

is the Green's function of the free phonons (M is the mass of the cell). The absorption of the sound will be determined by the imaginary part of $\Pi(\mathbf{k}, \Omega)$.

Let us consider the absorption of sound in the case when its frequency satisfies the condition $\Omega t_S \gg 1$, where $t_S$ is the characteristic magnon relaxation time. The magnon relaxation time for the case $1/r_0^3\sqrt{\tau} \ll 1$, when the technique in question is valid, was obtained in [7] and is given by the expression $t_S^{-1} \sim T\ln\tau/r_0^3\sqrt{\tau}$, where $\tau = (\Theta_C - T)/\Theta_C$, and therefore the frequency of the sound should satisfy the inequality

$$\Omega/T \gg \ln\tau/r_0^3\sqrt{\tau}.$$

Since the period of the sound wave is smaller than the relaxation time, we can disregard completely the relax-

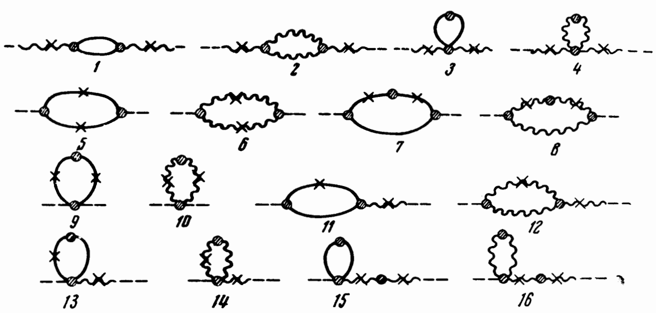


FIG. 2. First-order diagrams for the irreducible self-energy part.

ation processes and regard the absorption of sound as merely the absorption of acoustic quanta by magnon excitations.

Assuming the average interaction radius to be large compared with the interatomic distance, let us consider the first term in the expansion of the self-energy part of $\Pi$ in powers of $r_0^{-3}$. In this case the irreducible self-energy part $\Pi_1$ will be equal to the sum of the expressions corresponding to diagrams with only one loop. Figure 2 shows these diagrams. The solid line corresponds to the effective interaction $V^{+-}(\mathbf{p}, i\omega_n)$, which joins the vertex $S^+$ with the vertex $S^-$ and satisfies the equation

$$V^{+-}(\mathbf{p}, i\omega_n) = V_\mathbf{p} + \beta V_\mathbf{p}^2 K^{+-}(\mathbf{p}, i\omega_n), \tag{6}$$

where $V_\mathbf{p} = \sum_\mathbf{r} V(\mathbf{r}) e^{i\mathbf{p}\cdot\mathbf{r}}$, and $K^{\alpha\beta}(\mathbf{p}, i\omega_n)$ is the temperature correlation function of the operators $S^\alpha$ and $S^\beta$, defined in [6]. A wavy line corresponds to the effective interaction $V^{zz}(\mathbf{p}, i\omega_n)$, which joins the vertices $S^z$ with one another and satisfies the equation

$$V^{zz}(\mathbf{p}, i\omega_n) = V_\mathbf{p} + \beta V_\mathbf{p}^2 K^{zz}(\mathbf{p}, i\omega_n). \tag{7}$$

The lines marked in Fig. 2 by crosses correspond to the interaction $\nabla_\mathbf{r} V(\mathbf{r} - \mathbf{r}')$ and differ from $V^{+-}(\mathbf{p}, i\omega_n)$ and $V^{zz}(\mathbf{p}, i\omega_n)$ by a factor $p\cos\alpha$, where $\alpha$ is the angle between the vector $\mathbf{p}$ and the phonon wave vector $\mathbf{k}$.

We present analytic expressions for the single-cell blocks $\Gamma_{n0}$, needed in the calculation of $\Pi_1$:

$$\Gamma_{20}^{zz}(\omega_1, \omega_2) = b'\delta_1\delta_2, \qquad \Gamma_{20}^{+-}(\omega_1, \omega_2) = bG(\omega_1)\delta_{1-2},$$

$$\Gamma_{30}^{+-z}(\omega_1, \omega_2, \omega_3) = -bG(\omega_1)G(\omega_2)\delta_{1-2-3} + b'G(\omega_1)\delta_{1-2}\delta_3,$$

$$\Gamma_{30}^{zzz}(\omega_1, \omega_2, \omega_3) = -b''\delta_1\delta_2\delta_3,$$

$$\Gamma_{40}^{+-zz}(\omega_1, \omega_2, \omega_3, \omega_4) = bG(\omega_1)G(\omega_2)[G(\omega_1+\omega_3) + G(\omega_1+\omega_4)]\delta_{1-2+3+4} + b''G(\omega_1)\delta_{1-2}\delta_3\delta_4 - b'G(\omega_1)G(\omega_2)[\delta_{1-2+3}\delta_4 + \delta_{1-2+4}\delta_3].$$

Here $\delta_{i-k} \equiv \delta(\omega_i - \omega_k)$ is the Kronecker symbol, and $b'$ and $b''$ are respectively the first and second derivatives of $b(y)$ with respect to $y$.

To study the singularities of $\Pi$, we need to investigate the difference $\Pi(\mathbf{k}, \Omega) - \Pi(\mathbf{k}, 0)$, where $\Pi(\mathbf{k}, 0) = \Pi(\mathbf{k}, i\Omega_m)|_{m=0}$. The blocks $\Gamma_{20}^{zz}$, $\Gamma_{30}^{zzz}$ and the second term in $\Gamma_{30}^{+-z}$ contain $\delta(\omega_j)$ as factors, where $\omega_j$ is the frequency corresponding to $V^{zz}(\mathbf{p}, i\omega_j)$. It is obvious that inasmuch as this frequency coincides with the phonon frequency $\Omega_m$ in the diagrams 2, 4, 12, 15, and 16 of Fig. 2, such diagrams need not be taken into account. Similar reasoning holds for the blocks $\Gamma_{nm}$ defined above. As a result, to obtain $\Pi_1(\mathbf{k}, \Omega) - \Pi_1(\mathbf{k}, 0)$, it is necessary to take into account only the diagrams 1, 3, 5, 7, 9, 11, and 13. Corresponding to them are the following expressions:

diagram 1

$$\frac{\beta^3\langle S\rangle^2 k^2 V_\mathbf{k}^2 b^2}{N} \sum_{\mathbf{p}, \omega_n} G^2(\omega_n) G^2(\omega_n + \Omega_m) V^{+-}(\mathbf{p} + \mathbf{k}, \omega_n + \Omega_m) V^{+-}(\mathbf{p}, \omega_n),$$

diagram 3

$$\frac{\beta^3\langle S\rangle^2 k^2 V_\mathbf{k}^2 b^2}{N} \sum_{\mathbf{p}, \omega_n} G^3(\omega_n) V_\mathbf{p} V^{+-}(\mathbf{p}, \omega_n)[G(\omega_n + \Omega_m) + G(\omega_n - \Omega_m)],$$

diagram 5

$$-\frac{2\beta b^2}{N} \sum_{\mathbf{p}, \omega_n} p\cos\alpha(p\cos\alpha + k) G(\omega_n) G(\omega_n + \Omega_m) \times V^{+-}(\mathbf{p}, \omega_n) V^{+-}(\mathbf{p} + \mathbf{k}, \omega_n + \Omega_m),$$

diagram 7 (8)

$$\frac{\beta^2 b^3}{N} \sum_{\mathbf{p}, \omega_n} G(\omega_n) G(\omega_n + \Omega_m) V^{+-}(\mathbf{p}, \omega_n) V^{+-}(\mathbf{p} + \mathbf{k}, \omega_n + \Omega_m) \times [p^2\cos^2\alpha V_\mathbf{p} G(\omega_n + \Omega_m) + (p\cos\alpha + k)^2 V_{\mathbf{p}+\mathbf{k}} G(\omega_n)],$$

diagram 9

$$\frac{\beta b^2}{N} \sum_{\mathbf{p}, \omega_n} p^2\cos^2\alpha V_\mathbf{p} G(\omega_n) V^{+-}(\mathbf{p}, \omega_n)[G(\omega_n + \Omega_m) + G(\omega_n - \Omega_m)],$$

diagram 11

$$\frac{2\beta^2\langle S\rangle k V_\mathbf{k} b^2}{N} \sum_{\mathbf{p}, \omega_n} G(\omega_n) G(\omega_n + \Omega_m) V^{+-}(\mathbf{p}, \omega_n) V^{+-}(\mathbf{p} + \mathbf{k}, \omega_n + \Omega_m) \times [p\cos\alpha G(\omega_n + \Omega_m) - (p\cos\alpha + k) G(\omega_n)],$$

diagram 13

$$\frac{2\beta^2\langle S\rangle k V_\mathbf{k} b^2}{N} \sum_{\mathbf{p}, \omega_n} p\cos\alpha G^2(\omega_n) V_\mathbf{p} V^{+-}(\mathbf{p}, \omega_n)[G(\omega_n + \Omega_m) - G(\omega_n - \Omega_m)].$$

Here $\Omega_m$ is the frequency of the external phonon line. Since $1/r_0^3\sqrt{\tau} \ll 1$, it follows, as shown in [6], that one can use for the average spin the value corresponding to the molecular-field approximation (3), $\langle S\rangle = b(y)$. Carrying out summation over $\omega_n$ in (8), making the analytic continuation $i\Omega_m \to \Omega + i\delta$, and adding the contributions of all the diagrams, we obtain

$$\Pi_1(\mathbf{k}, \Omega) = \frac{b^2 v_c T}{16\pi^3 \Theta_c} \int d^3p [kV_\mathbf{k} + p\cos\alpha V_\mathbf{p} - (p\cos\alpha + k) V_{\mathbf{p}+\mathbf{k}}]^2 \frac{\operatorname{cth}(\varepsilon_\mathbf{p}/2T) - \operatorname{cth}(\varepsilon_{\mathbf{p}+\mathbf{k}}/2T)}{\varepsilon_{\mathbf{p}+\mathbf{k}} - \varepsilon_\mathbf{p} - \Omega - i\delta}, \tag{9}$$

where $v_c$ is the value of the elementary cell, and $\epsilon_\mathbf{p} = b(y)(V_0 - V_\mathbf{p}) + \mu H$ is the energy of the spin wave in the zeroth approximation in $1/r_0^3\sqrt{\tau}$. Obviously, $\operatorname{Im}\Pi_1(\mathbf{k}, \Omega)$ exists only for $\Omega \lesssim \epsilon_{\mathbf{p}+\mathbf{k}} - \epsilon_\mathbf{p} \sim bV_0R_0k$. In our case $\Omega = sk$ ($s$ is the speed of sound) and $bV_0 \sim \Theta_C\sqrt{\tau}$, and therefore when $\tau \gtrsim \Theta_0/r_0\Theta_C$ the principal role in the attenuation of the sound should be played by the long-wave magnons ($\Theta_0$ is the corresponding characteristic temperature). The potential $V_\mathbf{p}$ can be represented in this case in the form

$$V_\mathbf{p} = V_0\left[1 - \frac{1}{2}\sum_{\alpha,\beta} p^\alpha p^\beta \sum_\mathbf{r} x_\alpha x_\beta \frac{V(\mathbf{r})}{V_0}\right] = V_0\left[1 - \frac{1}{2}\sum_{i=1}^{3} (p^i)^2 x_{0i}^2\right]. \tag{10}$$

Here $x_{0i}^2$ are the principal values of the tensor $V_0^{-1}\Sigma_\mathbf{r} x_\alpha x_\beta V(\mathbf{r})$, and $p^i$ is the projection of the vector $\mathbf{p}$. For cubic lattices, for example, we have $x_{0i}^2 = R_0^2/3$.

Taking (10) into account, let us calculate Im $\Pi_1(\mathbf{k}, \Omega)$ at $T \sim \Theta_C$. For simplicity we consider the case of a zero external field. As a result we have for the damping

$$\gamma = \frac{9\sqrt{3}}{16\pi r_0^4 y}\frac{\Theta_0}{Ms^2}\left(\frac{T}{\Theta_c}\right)^2 \Omega \left\{1 - \left(\frac{2m^2\Omega^2}{k^2} - k^2 - m\Omega\right)^2 + 2\left(\frac{2m^2\Omega^2}{k^2} - k^2\right)\ln\frac{4k^2}{|4m^2\Omega^2 - k^4|} + \frac{[(2m^2\Omega^2/k^2 - k^2)^2 + m^2\Omega^2]}{m\Omega}\ln\left|\frac{2m\Omega + k^2}{2m\Omega - k^2}\right|\right\}, \tag{11}$$

where $m = 1/bV_0$, $k = kR_0$, and $y \sim \sqrt{\tau}$. The expression in the curly brackets is of the order of unity for all $k \lesssim 1/R_0$, and the damping is given in this case by the formula

$$\gamma \sim \frac{1}{r_0^4\sqrt{\tau}}\frac{\Theta_0}{Ms^2}\left(\frac{T}{\Theta_c}\right)^2 \Omega. \tag{11'}$$

It is seen from (11′) that the damping of the sound increases on approaching the transition point. This is due to the fact that near $\Theta_C$ the density of the spin waves increases. In the immediate vicinity of the transition point, our analysis does not hold, for in this case it is necessary to take into account the growth of the damping of the spin waves and the scattering by the fluctuations of the momentum $S^z$.

A comparison of the sound damping (11′) obtained by us with the case of low temperatures $T \ll \Theta_C$, considered in [3], where

$$\gamma \sim \frac{\Theta_0}{Ms^2}\left(\frac{T}{\Theta_c}\right)^2 \Omega, \tag{12}$$

shows that when $\tau \sim 1$ the temperature and frequency dependences of the damping practically coincide. This is natural, for in either case the damping is determined by the spin waves.

Sound absorption as the result of the phonon-phonon interaction was considered in [8,9]. It was shown that in the region of temperatures and frequencies of interest to us it takes the form

$$\gamma \approx \Omega\frac{\Theta_0}{Ms^2}\left(\frac{T}{\Theta_0}\right)^4 \tag{13}$$

for high-temperature ferrodielectrics ($\Theta_C > \Theta_0$) and

$$\gamma \approx \Omega^2\frac{1}{Ms^2}\left(\frac{T}{\Theta_C}\right) \tag{14}$$

for low-temperature ferrodielectrics ($\Theta_C > \Theta_0$).

It is seen from formulas (13), (14), and (11′) that the considered magnetic absorption of sound is small compared with the absorption due to phonon-phonon interaction in low-temperature dielectrics and becomes appreciable in high-temperature ferrodielectrics when

$$\sqrt{\tau} \sim \left(\frac{\Theta_0}{r_0\Theta_C}\right)^4\frac{\Theta_C}{\Omega}.$$

It should be noted in conclusion that in ferrodielectrics the interaction radius, which we assumed to be large, is usually small ($r_0 \approx 3$–$4$). One can hope, however, that the present paper gives a correct qualitative description.

The author is grateful to V. L. Pokrovskiĭ, S. A. Pikin, and L. D. Romelashvili for useful discussions.

[1] A. I. Akhiezer, J. Phys. USSR **10**, 217 (1946).

[2] M. I. Kaganov and V. M. Tsukernik, Zh. Eksp. Teor. Fiz. **36**, 224 (1959) [Sov. Phys.-JETP **9**, 151 (1960)].

[3] M. I. Kaganov and Ya. M. Chikvashvili, Fiz. Tverd. Tela **3**, 275 (1961) [Sov. Phys.-Solid State **3**, 200 (1961)].

[4] A. I. Akhiezer and A. A. Shishkin, Zh. Eksp. Teor. Fiz. **34**, 1267 (1958) [Sov. Phys.-JETP **7**, 875 (1958)].

[5] B. I. Shklovskiĭ, Fiz. Tverd. Tela **9**, 1917 (1967) [Sov. Phys.-Solid State **9**, 1512 (1968)].

[6] V. G. Vaks, A. I. Larkin, and S. A. Pikin, Zh. Eksp. Teor. Fiz. **53**, 281 (1967) [Sov. Phys.-JETP **26**, 188 (1967)].

[7] V. G. Vaks, A. I. Larkin, and S. A. Pikin, ibid. **53**, 1089 (1967) [**26**, 647 (1968)].

[8] L. D. Landau and G. Rumer, Zs. Phys. Sowjet **11**, 18 (1937).

[9] L. E. Gurevich and B. I. Shklovskiĭ, Fiz. Tverd. Tela **9**, 526 (1967) [Sov. Phys.-Solid State **9**, 401 (1967)].

[10] A. A. Abrikosov, L. P. Gor'kov, and I. E. Dzyaloshinskiĭ, Metody kvantovoĭ teorii polya v statisticheskoĭ fizike (Quantum Field Theoretical Methods in Statistical Physics), Fizmatgiz, 1962 [Pergamon, 1965].

Translated by J. G. Adashko
255